CRYSTAL GROWTH & DESIGN

Article

pubs.acs.org/crystal

Influence of the Molecular Groups Ordering on Structural Phase Transitions in $(NH_4)_2WO_2F_4$ Crystal

Published as part of the Crystal Growth & Design virtual special issue Anion-controlled New Inorganic Materials.

Alexander S. Krylov,[†] Sergey V. Goryainov,[‡] Natalia M. Laptash,[§] Alexander N. Vtyurin,[†] Svetlana V. Melnikova,[†] and Svetlana N. Krylova*[,†]

[†]Kirensky Institute of Physics SB RAS, Krasnoyarsk 660036, Russia

[‡]Institute of Geology and Mineralogy SB RAS, Novosibirsk 630090, Russia

[§]Institute of Chemistry FEB RAS, Vladivostok 690022, Russia

ABSTRACT: Phase transitions of the $(NH_4)_2WO_2F_4$ crystal were studied by Raman spectroscopy in the range from 10 to 350 K. The mechanism of two phase transitions at T_1 = 201 and T_2 = 160 K was proposed. The significant spectra changes occur in the range corresponding to the W−O vibrations. The first temperature phase transition is due to the ordering of the quasi-octahedral groups $[WO_2F_4]^{2-}$ and partial ordering of ammonium groups. Experimental data allow for attributing the first (T_1 = 201 K) phase transition to the first order close to the tricritical point. The noticeable changes of the Raman spectrum have been found in the range corresponding to the ammonium vibrations below the temperature T_2. The second phase transition is associated with the further ordering of ammonium groups. Room temperature (296 K) experiments have been carried out under high hydrostatic pressure up to 10 GPa. Above 2 GPa, new spectral features appear, allowing for the assumption of the existence of a new high-pressure phase of $(NH_4)_2WO_2F_4$, which is mainly connected with ordering of the $[WO_2F_4]^{2-}$ quasi-octahedral groups.

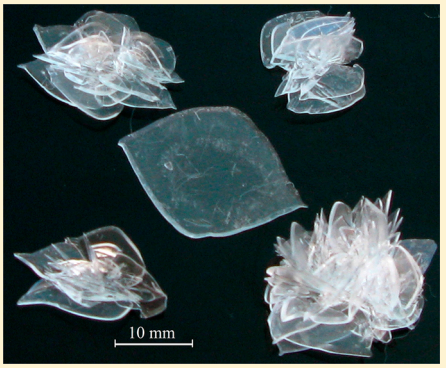

INTRODUCTION

Noncentrosymmetric building units with individual net dipole moments are extensively used in solid-state chemistry for the engineering of new materials with interesting properties (piezoelectricity, nonlinear optics, ferroelectricity, pyroelectricity, etc.).

Crystals with the common formula of $A_2MO_2F_4$ (A = Na, Rb, Cs, or NH_4, M = W and Mo) attract our attention due to the presence of noncentrosymmetric quasi-octahedral anions $[MO_2F_4]^{2-}$. These are characterized by a relatively simple crystal lattice structure and sufficient flexibility, allowing one to widely change a set of lattice-forming ions and to achieve a necessary combination of material properties. This enables one to create structures, with macroscopic dipole moment appearing by itself or due to external effects.[1,2] Besides the possibility of obtaining ferroelectric and ferroelastic states in oxyfluorides, there are other factors, making these materials more attractive for practical applications. A high level of ionic group disorder in highly symmetrical phases, phase transitions accompanied by significant entropy changes, and the sensitivity of the phase transitions to external pressure allow one to consider oxyfluorides as promising materials to achieve barocaloric effects.[3] This offers new perspectives for using these compounds as active elements of solid-state coolers.[4]

The crystal structure of diammonium dioxotetrafluorotungstate $(NH_4)_2WO_2F_4$ is orthorhombic at room temperature: G_0 = $Cmcm$, Z = 4.[5,6] It consists of isolated quasi-octahedra $[WO_2F_4]^{2-}$ of *cis*-configuration. Two independent states of *cis*-WO_2F_4 octahedron are characteristic of static and dynamic disorder in this structure. Two crystallographically independent ammonium groups, $N1H_4$ and $N2H_4$, reorient independently from octahedra.[7]

With the temperature decreasing, the crystal undergoes two subsequent phase transitions $G_0 \rightarrow G_1 \rightarrow G_2$ at temperatures T_1 = 201 K and T_2 = 160 K.[5] The entropy changes accompanying the phase transitions appear to be significantly different: ΔS_1 = 19.0 J/mol·K($\sim R$ ln 10) and ΔS_2 = 1.4 J/mol·K (R ln 1.2).[5] The authors suggest that the high temperature transition is associated with the processes of ordering of the structural elements, while the low temperature one is due to small atomic displacements in an already ordered phase. The structure of the distorted phase G_1 of $(NH_4)_2WO_2F_4$ is triclinic $P\bar{1}$, Z = 4.[7] Below T_2 the structure of $(NH_4)_2WO_2F_4$ is also characterized by triclinic symmetry ($P\bar{1}$). As for the ammonium tetrahedra, it is assumed they are not fully ordered. Thermal expansion, phase diagrams, and barocaloric effect for this crystal were studied.[6] The complex analysis of the crystal structure and entropy changes[5,6] allows one to assume that the phase transition mechanism at T_1 can include the ordering of both quasi-octahedra

Received: June 14, 2013
Revised: November 13, 2013
Published: December 2, 2013

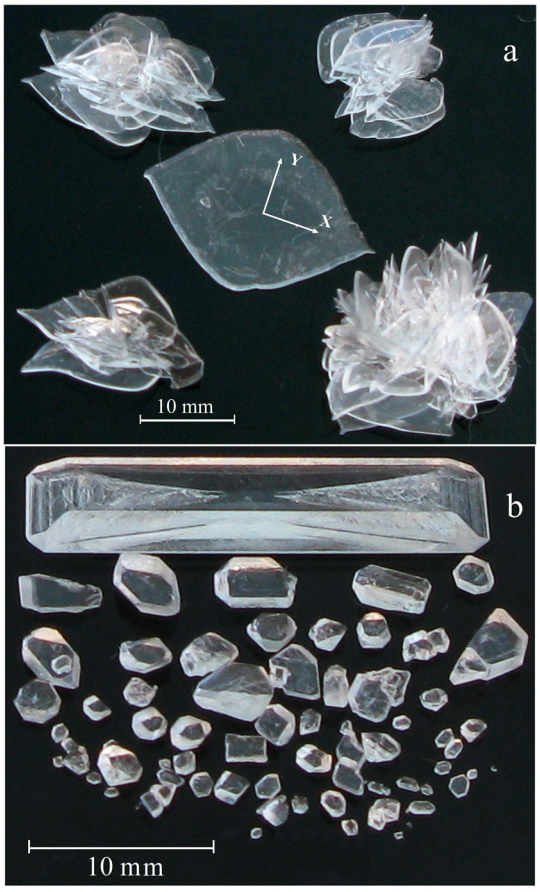

Figure 1. Flower-like druses of the $(NH_4)_2WO_2F_4$ plates obtained from (a) scheelite and single crystals obtained through (b) intermediate $(NH_4)_3WO_3F_3$.

(and, correspondingly, that of the central atom) and ammonium tetrahedra. The phase transitions of $(NH_4)_2WO_2F_4$ in the range from 10 to 300 K were studied by the method of incoherent inelastic scattering.[8] The investigation confirmed the hypothesis on the contribution of the tetrahedra ordering into the entropy change of the high-temperature phase transition.

Thus, two structural phase transitions in the $(NH_4)_2WO_2F_4$ crystal were considered by earlier studies.[5,9] No considerable structural differences between the intermediate G_1 and low-temperature G_2 distorted phases were observed. The phase transition mechanism at T_2 was not determined. It was established that the temperature range of the intermediate phase stability decreased with increasing hydrostatic pressure. However, no studies were performed at a pressure above 0.6 GPa.

Further investigations of structural changes in the crystal $(NH_4)_2WO_2F_4$ are necessary to specify the mechanisms and phase transitions. The method of Raman spectroscopy can be an additional powerful tool for studying phase transitions. This method allows one to estimate the role of molecular groups in the phase transition mechanism and character of phase transitions. In particular, temperature and baric phase transitions in other oxyfluorides[10−13] were studied by Raman spectroscopy. The present paper describes the temperature- and pressure-dependent structural changes in $(NH_4)_2WO_2F_4$ by using Raman spectroscopy to clarify the phase transition mechanisms.

EXPERIMENTAL SECTION

Tungsten oxide compounds, aqueous hydrofluoric acid (45% HF by weight), and ammonium hydrogen difluoride (NH_4HF_2) of a reagent grade were used. The compound under investigation was prepared in two ways. The first one was the fluorination of tungstates with concentrated HF at heating. It is a conventional method used by Marignac, as early as 1862.[14] We used WO_3 or ammonium paratungstate, but the recovery degree (the yield based on W) was not more than 70%. So, we suggest the more productive, suitable, and faster way comprising the interaction of two solids: calcium tungstate (scheelite) $CaWO_4$ and ammonium hydrogen difluoride NH_4HF_2.[15] The initial components were mixed in a stoichiometric ratio and heated to 150−200 °C for 0.5−1.0 h, yielding $(NH_4)_3WO_2F_5$ with a virtually 100% yield. The reaction is exothermic and takes place even at room temperature:

$$CaWO_4 + 3.5NH_4HF_2 = CaF_2 + (NH_4)_3WO_2F_5 + 0.5NH_3 + 2H_2O$$

The cake was leached with water (solid: liquid = 1:4), and insoluble CaF_2 was precipitated. The mother liquor was filtered and slowly evaporated in air. $(NH_4)_2WO_2F_4$ was crystallized from the saturated solution in the form of plates forming flowerlike druses (Figure 1a). High-quality, variously shaped single crystals (thick plates, prisms, and isometric polyhedra) of this salt were obtained through $(NH_4)_3WO_3F_3$, which was precipitated from a hot solution of $(NH_4)_2WO_2F_4$ in the excess of NH_4F followed by the addition of aqueous NH_3, until a white product appeared during the stirring process. The solid was dissolved in HF aqueous solution, filtered, and slowly evaporated in air at room temperature. The size of prismatic single crystals was from 0.2 to 25 mm in length (Figure 1b).

Raman spectra were acquired using a Horiba Jobin Yvon T64000 spectrometer in backscattering geometry, operating in the dispersion subtraction mode with the spectral resolution determined by the entrance slit of 2 cm^{-1} (the resolution was achieved using a 100 μm slit diffraction grating with 1800 line/mm). The spectra were excited using an Ar+ laser (wavelength of 514 nm) with the power of 20 mW, corresponding to a laser power density of 60 W/cm^2. Temperature measurements were taken by a closed-cycle helium cryostat ARS CS204-X1.SS. The temperature was controlled using a calibrated

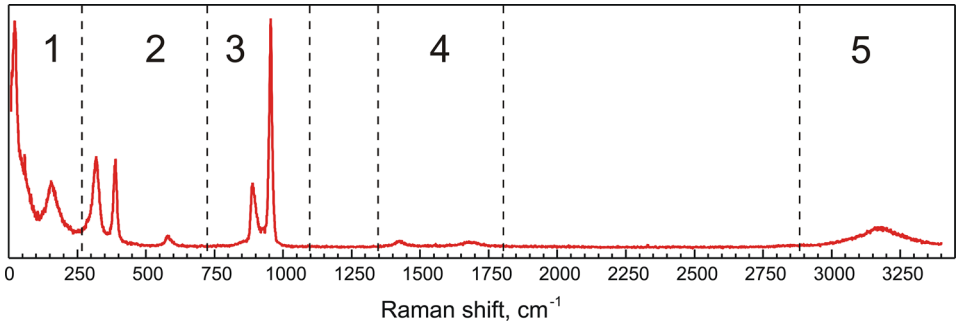

Figure 2. Raman spectrum of crystal $(NH_4)_2WO_2F_4$ at 295 K.

dx.doi.org/10.1021/cg400899m | Cryst. Growth Des. 2014, 14, 374−380

Table 1. Experimental and Calculated Vibrational Wavenumbers of the $[WO_2F_4]^{2-}$ Anion

Raman experiment $(NH_4)_2WO_2F_4$ at 295 K (the present work), cm^{-1}		calculation $[WO_2F_4]^{2-}$ (C_{2v}) DFT/B3LYP (cm^{-1})[23]		IR experiment, wavenumber (cm^{-1})[24]			
wavenumber (cm^{-1})	FWHM (cm^{-1})	wavenumber (cm^{-1})	assignment	$K_2WO_2F_4$	$Rb_2WO_2F_4$	$Cs_2WO_2F_4$	assignment
955	12	939	$\nu_s(WO_2)$	910	955	946	WO_2
898 888	27 13	886	$\nu_{as}(WO_2)$	880	904	892	WO_2
579	19	542	$\nu_s(WF_{c2}) + \nu_s(WF_{t2})$		574	570	WF
387	15	373	$\delta(WO_2)$				
317	26	304	$\omega(WO_2)$				
161	62	179	$\delta(WF_{c2}) + \tau\ (WO_2 - WF_{t2})$				

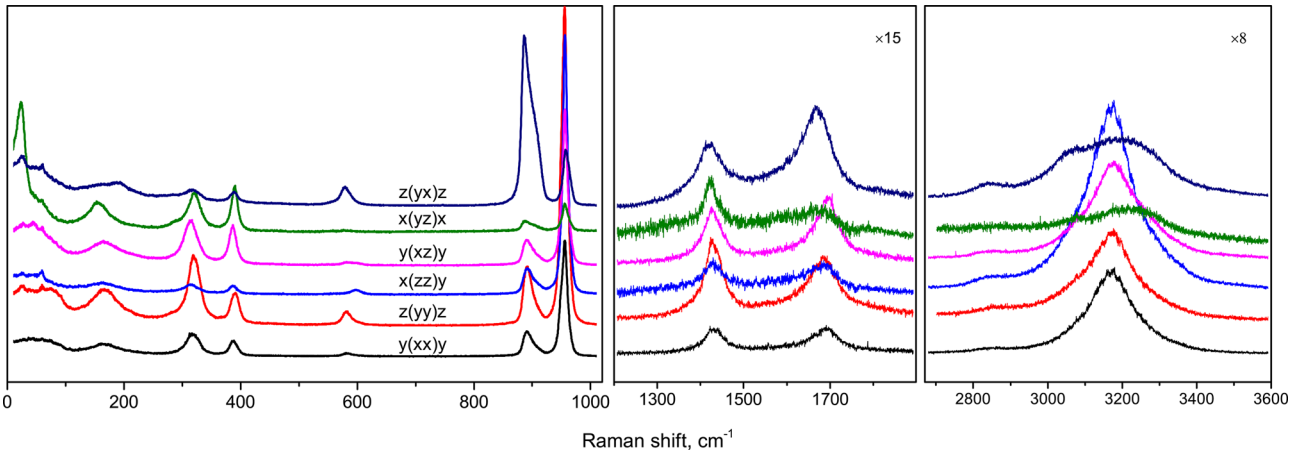

Figure 3. Polarized Raman spectra of the crystal.

silicon diode LakeShore DT-6SD1.4L. The temperature stabilization accuracy was better than 0.2 K. The sample was placed in the indium gasket, with one side being opened and then mounted on the cold finger. During the experiments, the cryostat was pumped to a pressure of 1.0×10^{-6} mBar.

The experiments were carried out under the conditions of high hydrostatic pressure at room temperature (295 K), using a diamond anvil cell with the sample chamber diameter of 0.25 mm and height of 0.2 mm. The pressure to the accuracy of 0.05 GPa was determined by the shift of the luminescence line $2F_g\ 4A_{2g}$ of the Cr^{3+}ion of a ruby microcrystal located near the sample.[15,16] A carefully dehydrated mixture of ethanol and methanol in the ratio 4:1 was used as a pressure-transmitting medium.[17−19]

To analyze quantitatively the temperature dependences of the low frequency part of the spectrum (up to 100 cm^{-1}), the damped harmonic oscillator function was used.[20,21] The other part was analyzed by using the Lorenz circuit.[22]

RESULTS AND DISCUSSION

The full spectrum of the crystal $(NH_4)_2WO_2F_4$ at 295 K is presented in Figure 2. A high degree of the ionic group disorder does not allow a full theoretical and group analysis. To interpret the spectra at room temperature, the evidence presented in ref 23 was used. Table 1 shows the experimental and simulated vibration spectra of the $[WO_2F_4]^{2-}$ group. The first column presents the results of the current experiment on Raman scattering at 295 in the crystal $(NH_4)_2WO_2F_4$. The second column shows the corresponding Raman scattering frequencies of the $[WO_2F_4]^{2-}$ ion in the $(NH_4)_2WO_2F_4$ crystal and their assignments.[23] The abbreviations denote stretch (ν), bend (δ), wag (ω), rock (τ), symmetric (s), and asymmetric (as). The corresponding frequencies of the IR absorption in oxyfluorides containing potassium, rubidium, and cesium cations in the outer sphere are given for comparison.[24] Such an interpretation allows one to conventionally divide the spectrum into 5 parts: 1, up to 150 cm^{-1} lattice vibrations; 2, in the range from 150 to 750, stretching W−F vibrations and

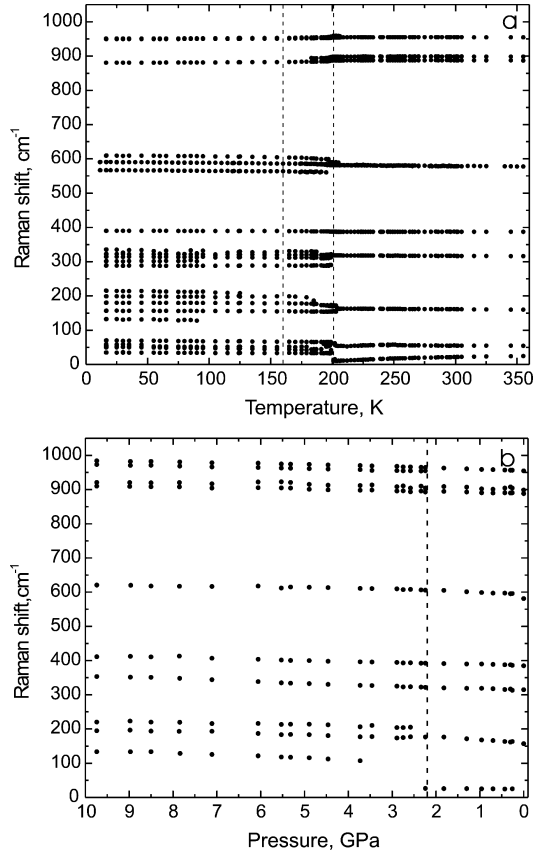

Figure 4. Dependencies of the line positions, a, on temperature and b, on pressure in the range from 0 to 1000 cm^{-1}.

dx.doi.org/10.1021/cg400899m | Cryst. Growth Des. 2014, 14, 374−380

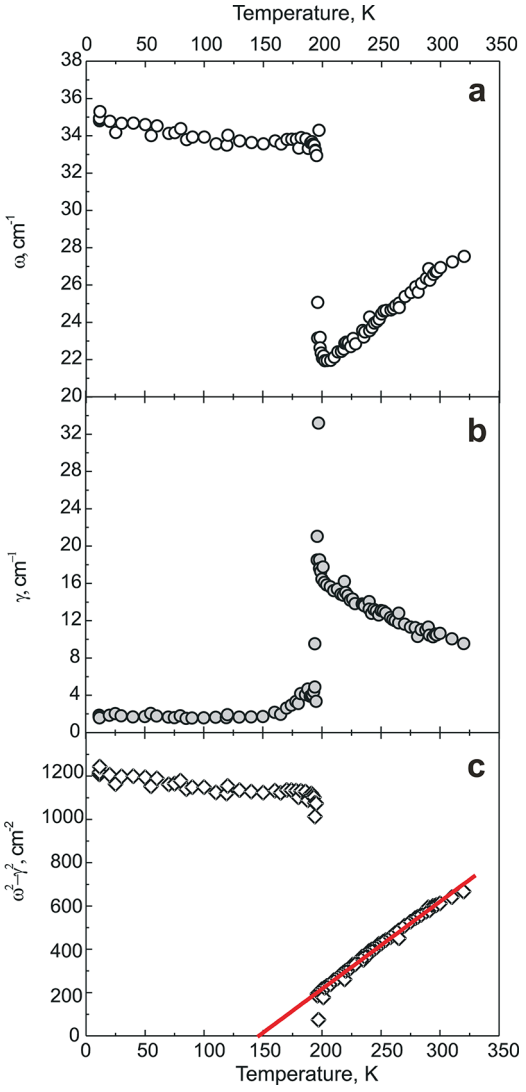

Figure 5. (a) Temperature dependence of the position of the low wavenumber mode, (b) temperature dependence of half width at half-maximum, and (c) temperature dependence of the effective wavenumber squared.

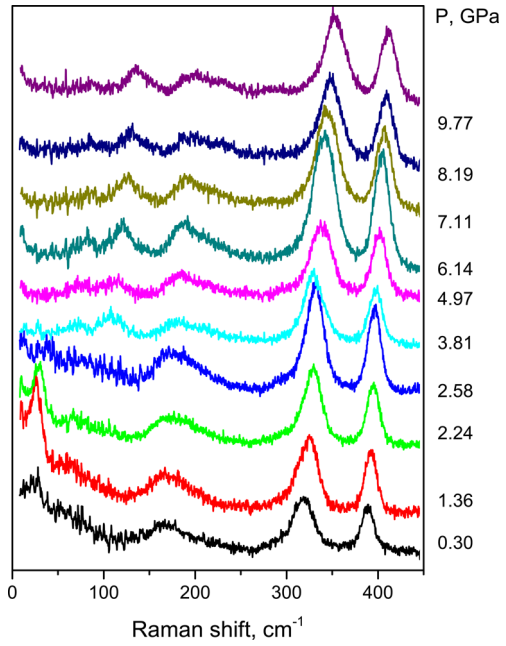

Figure 6. Transformation of low wavenumber part of spectrum under increasing pressure.

bending O(F)−W−O(F) vibrations of the $[WO_2F_4]^{2-}$ ions; 3, in the range from 750 to 1100 cm^{-1}, stretching W−O vibrations of the $[WO_2F_4]^{2-}$ ions; 4, in the range from 1200 to 1800 cm^{-1}, ammonium bending vibrations; 5, in the range from 2500 cm^{-1} to 3500 cm^{-1}, ammonium stretching vibrations are observed.

An overview of the experimental polarized Raman spectra for all components of Raman tensor at room temperature 296 K is shown in Figure 3.

Temperature measurements were taken in the temperature range of 8−350 K. The behavior of the temperature dependence of the line position in the range up to 1000 cm^{-1} is given in Figure 4a. In the range from 100 to 650 cm^{-1}, one can observe the stretching and bending vibrations of W−F at 575 cm^{-1} and 162 cm^{-1}, as well as the bending vibrations of O−W−O at 387 and 317 cm^{-1}. Up to the temperature T_1 = 201 K, the positions of all the lines behave monotonically (Figure 4a). New modes appear after the transition from orthorhombic into the triclinic phase (T_1 = 201 K). However, no anomalies in the spectra are observed associated with the second phase transition (T_2 = 160) in the range of the lattice vibrations, stretching vibrations W−F, and bending ones O−W−O. In the range from 40 to 100 cm^{-1}, a mode at 55 cm^{-1} is observed at 350 K. New lines appear below 200 K, the line positions are distinctly shifted, and the slope of the temperature dependencies of the positions of some lines changes. The wavenumber shift of the line at 55 cm^{-1} amounts to 15 cm^{-1}. An abrupt change of the wavenumber indicates that the first transition is of the first order. The anomalous behavior of the lowest wavenumber mode (28 cm^{-1} at 350 K) in this range deserves particular consideration. The changes of the positions of the spectral lines in the range from 10 to 1000 cm^{-1} with increasing pressure are shown in Figure 4b. There appears a new line in the range of 200 cm^{-1}. The mode line at 25 cm^{-1} disappears at a pressure higher than 2 GPa. In the range up to 850 cm^{-1}, the number of lines in the low-temperature phase does not correspond to the number of lines in the high-pressure phase (Figure 4, panels a and b).

Figure 5 shows the temperature dependence of the position of the low wavenumber mode, the behavior of the half-width of the line width with temperature and square of the wavenumber $\omega^2 \equiv \omega^2_0 - \gamma^2$.[25] Figure 5c shows the soft mode position as a function of temperature. Good linear approximation, as evidenced by Figure 5c is typical for soft modes corresponding to phase transitions near tricritical points. The dependence obtained is approximated by the linear function, with the ordinate axis intercept being −591 cm^{-1} and the slope at 4.3 cm^{-1}/K. At 200 K, the line position increases by a jump from 22 to 34 cm^{-1} (Figure 5a). The line width at 200 K increases from 17 to 34 cm^{-1} and decreases abruptly to 5 cm^{-1} (Figure 5b). Such an abrupt change of the wavenumbers and linewidths indicates that there is a first-order phase transition. The similar behavior of the line width is observed in the oxyflouride $Rb_2KMoO_3F_3$ in the first-order transition.[13]

The low wavenumber modes can be connected with vibration of heavy ion (W) and lattice vibration. Transformation of

dx.doi.org/10.1021/cg400899m | Cryst. Growth Des. 2014, 14, 374−380

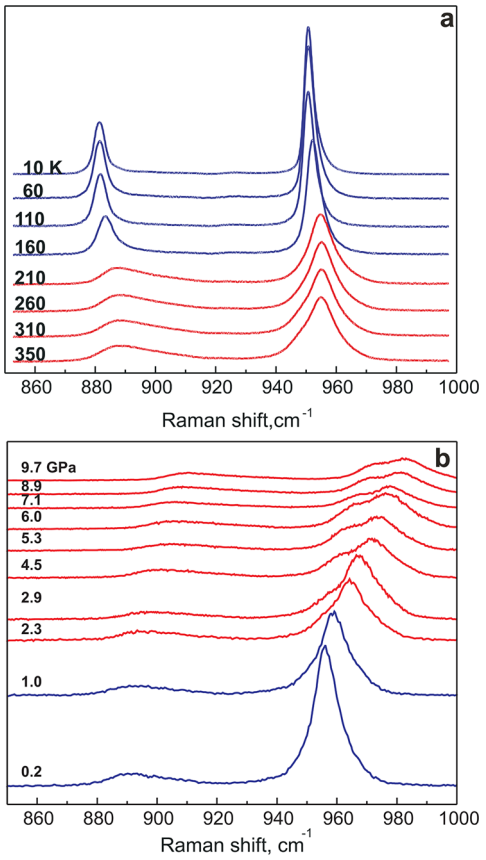

Figure 7. Spectrum transformation upon changing external parameters (a) temperature and (b) pressure in the range from 850 to 1000 cm^{-1}.

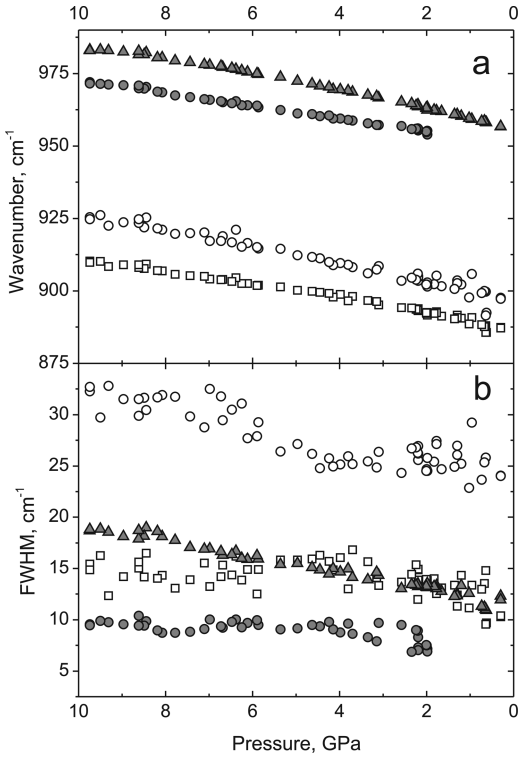

Figure 8. (a) Pressure dependence of line positions, (b) pressure dependence of the full width at half-maximum in the range of 875–1000 cm^{-1}.

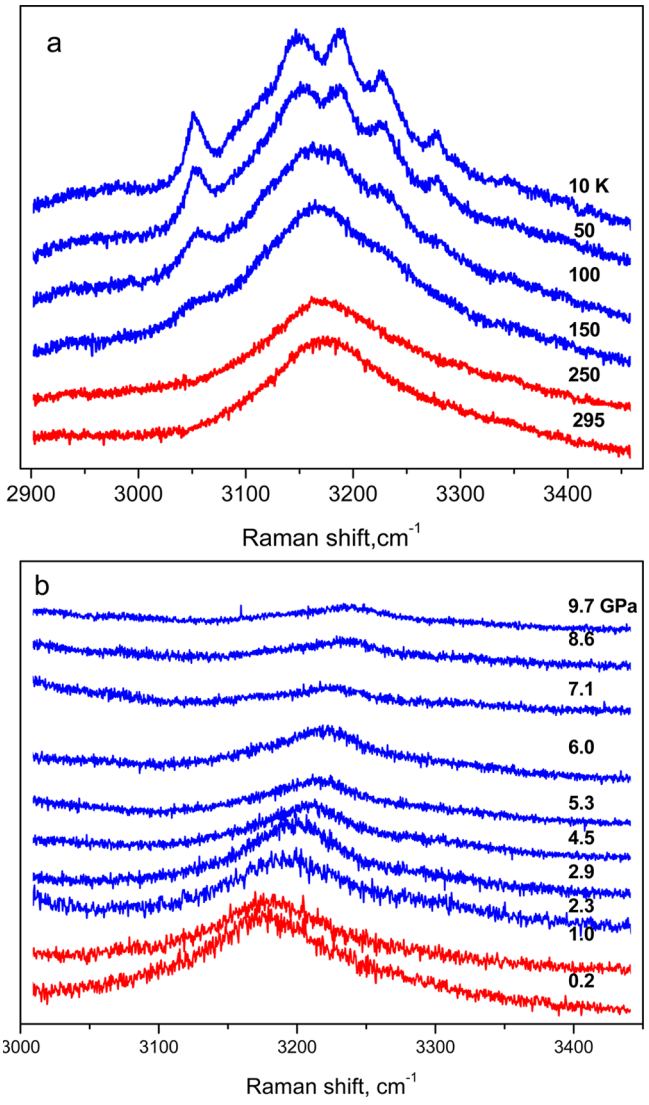

Figure 9. Spectra transformation with changing external parameters (a) temperature and (b) pressure in the range from 3000 to 3500 cm^{-1}.

the low wavenumber part of the spectrum under pressure increasing is presented in Figure 6. One can see significant changes in this part of the spectrum. The low wavenumber mode disappears (25 cm^{-1}) and new modes arrive under increasing pressure.

In the range from 860 to 1000 cm^{-1} one can observe the W–O stretching vibrations. The changes of this part of the spectrum with temperature are shown in Figure 7a. Cooling results in the lines becoming significantly narrowed, with one of them disappearing after the transition (T_1 = 201 K). A significant change of the line width confirms the assumption of there being the transition of the first order. In the wavenumber range to 1000 cm^{-1}, no anomalies associated with the second phase transition are observed. The high-pressure phase differs significantly from the low-temperature phase. With the temperature decreasing below 200 K, a line in the range of 890 cm^{-1} disappears (Figure 7a), while with increasing pressure there remain two lines in this range (Figure 7b).

There are also significant changes in the spectra in the range from 800 to 1000 cm^{-1}. Figure 8 shows the changes in the spectra with pressure in the range of 900 cm^{-1}. A new line appears in the range of W–O (950 cm^{-1}) vibrations at a

dx.doi.org/10.1021/cg400899m | Cryst. Growth Des. 2014, 14, 374–380

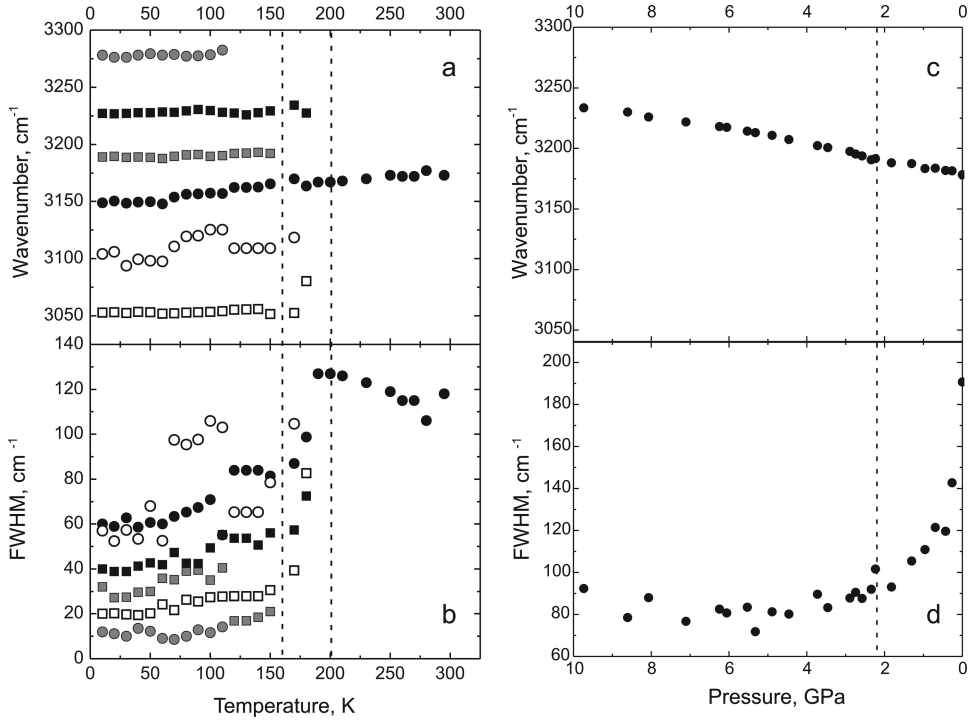

Figure 10. Dependence of the line positions (a) on temperature and (c) on pressure in the range from 3000 to 3300 cm^{-1}. Dependence of the full width at half-maximum on (b) temperature and (d) pressure in the range from 3000 to 3300 cm^{-1}.

pressure of 2 GPa. This vibration is fully symmetrical. Therefore, the appearance of a new line at baric transition can be due to the doubling of the unit cell volume. The observed phase transition appears in the ranges, corresponding to the lattice vibrations, stretching vibrations W−F and W−O, and bending vibrations O−W−O of the $WO_2F_4^{2-}$ ions.

The normal modes of vibration of a free NH_4^+ ion of Td symmetry have wavenumbers of 1397 (F_2), 1680 (E), 3040 (A_1), and 3145 (F_2) cm^{-1} modes.[26] The modes of the ammonium vibrations are of very low intensive (Figure 2). We could only analyze the F_2 symmetry stretching mode of ammonium. We expected the splitting of the triply degenerated stretching mode at 3150 cm^{-1} (F_2) in the low-symmetry phases. The changes in the spectra of the ammonium ion stretching vibrations with temperature are given in Figure 9a. With increasing pressure, the spectral line profile features hardly change (Figure 9b), while with the temperature decreasing below T_2, the spectral profile becomes complex (Figure 9a). However, the main changes in the range of the ammonium vibrations occur at temperatures below the second-phase transition (Figure 10). The spectral changes in the range of the ammonium stretching vibrations with temperature increasing are given in Figure 10 (panels a and b). Large linewidths, particularly in the range of 2500−3500 cm^{-1}, corresponding to the internal stretching vibrations of the ammonium ion, can be due to both the influence of the well-known anharmonicity of NH_4^+ ion vibrations[27] and the orientational disordering of ammonium sublattices.[26] New lines arise after decreasing temperature below T = 190 K. The phenomena observed can be accounted for by the fact that cooling the crystal below the phase transition temperature results in the ordering of the ammonium groups. The spectral changes with increasing pressure in the range of the ammonium ion stretching vibrations are given in Figure 10 (panels c and d). The position of the peak near 3150 cm^{-1} increases between 0 and 10 GPa (Figure 10c), while its width monotonically decreases from 190 to 85 cm^{-1} and becomes nearly constant above 2 GPa (Figure 10d). These spectral changes are connected with ordering processes of the ammonium group up to 2 GPa. Nearly constant bandwidth above 2 GPa shows that between 2 and 10 GPa ordering processes of ammonium group are not observed.

CONCLUSION

A new high-pressure phase of $(NH_4)_2WO_2F_4$ has been found at 2 GPa. The character of the changes in the $(NH_4)_2WO_2F_4$ spectra indicates that the high-pressure phase and low-temperature phase are different. The high-pressure phase transition is connected with the ordering of the $[WO_2F_4]^{2-}$ ions and partial ordering of the ammonium group. Splitting of the lines in the high-pressure phase in $(NH_4)_2WO_2F_4$ would indicate that the cell volume doubles.

The phase transition T_1 is of the first-order, close to the tricritical point. The molecular and ammonium ions in the high-temperature phase are disordered orientationally, which is evidenced by wide internal lines and weak temperature dependence of these widths far from the transition point T_1. The temperature phase transition T_1 is due to the ordering of the molecular groups of $[WO_2F_4]^{2-}$ and ammonium groups, while the phase transition T_2 is due to the ammonium ordering.

AUTHOR INFORMATION

Corresponding Author

*E-mail: slanky@iph.krasn.ru.

Funding

This work was partly supported by the Russian Foundation for the Basic Research project no. 12-02-00056, no. 13-02-00825, and integration project SB RAS no. 28, SS-4828.2012.2.

Notes

The authors declare no competing financial interest.

■ ACKNOWLEDGMENTS

The authors are grateful to Prof. I. N. Flerov for valuable support and useful discussions.

■ REFERENCES

(1) Heier, K. R.; Norquist, A. J.; Halasyamani, P. S.; Duarte, A.; Stern, C. L.; Poeppelmeier, K. R. *Inorg. Chem.* **1999**, *38*, 762−767.
(2) Marvel, M. R.; Lesage, J.; Baek, J.; Halasyamani, P. S.; Stern, C. L.; Poeppelmeier, K. R. *J. Am. Chem. Soc.* **2007**, *129*, 13963−13969.
(3) Flerov, I. N.; Gorev, M. V.; Tressaud, A.; Laptash, N. M. *Crystallogr. Rep.* **2011**, *56*, 9−17.
(4) Oliveira, N. A. *J. Appl. Phys.* **2011**, *109*, 053515.
(5) Flerov, I. N.; Fokina, V. D.; Gorev, M. V.; Vasiliev, A. D.; Bovina, A. F.; Molokeev, M. S.; Kocharova, A. G.; Laptash, N. M. *Phys. Solid State* **2006**, *48* (4), 759−764.
(6) Gorev, M. V.; Bogdanov, E. V.; Flerov, I. N.; Kocharova, A. G.; Laptash, N. M. *Phys. Solid State* **2010**, *52* (1), 167−175.
(7) Udovenko, A. A.; Laptash, N. M. *Acta Crystallogr.* **2008**, *B64*, 645−651.
(8) Smirnov, L. S.; Kolesnikov, A. I.; Flerov, I. N.; Laptash, N. M. *Phys. Solid State* **2009**, *51* (11), 2362−2366.
(9) Novak, D. M.; Smirnov, L. S.; Kolesnikov, A. I.; Voronin, V. I.; Berger, I. F.; Laptash, N. M.; Vasil'ev, A. D.; Flerov, I. N. *Crystallogr. Rep.* **2013**, *58* (1), 129−134.
(10) Krylov, A. S.; Goryainov, S. V.; Vtyurin, A. N.; Krylova, S. N.; Sofronova, S. N.; Laptash, N. M.; Emelina, T. B.; Voronov, V. N.; Babushkin, S. V. *J. Raman Spectrosc.* **2012**, *43*, 577−582.
(11) Krylov, A. S.; Krylova, S. N.; Vtyurin, A. N.; Laptash, N. M.; Kocharova, A. G. *Ferroelectrics* **2012**, *430*, 65−70.
(12) Krylov, A. S.; Vtyurin, A. N.; Fokina, V. D.; Goryainov, S. V.; Kocharova, A. G. *Phys. Solid State* **2006**, *48* (6), 1064−1066.
(13) Krylov, A. S.; Merkushova, E. M.; Vtyurin, A. N.; Isaenko, L. I. *Phys. Solid State* **2012**, *54* (6), 1275−1280.
(14) Marignac, M. C. *Ann. Chim. Phys.* **1863**, *69*, 61−86; *C. R. Acad. Sci.,* **1862**, *55*, 888−892.
(15) Laptash, N. M.; Melnichenko, E. I.; Polyshchuk, S. A.; Kaidalova, T. A. *J. Therm. Anal.* **1992**, *38*, 2335−2341.
(16) Munro, R. G.; Piermarini, G. J.; Block, S.; Holzapfel, W. B. *J. Appl. Phys.* **1985**, *57*, 165.
(17) Vos, W. L.; Schouten, J. A. *J. Appl. Phys.* **1991**, *69*, 6744.
(18) Piermarini, G. J.; Block, S.; Barnett, J. D. *J. Appl. Phys.* **1973**, *44* (12), 5377−5382.
(19) Goryainov, S. V.; Krylov, A. S.; Pan, Y.; Madyukov, I. A.; Smirnov, M. B.; Vtyurin, A. N. *J. Raman Spectrosc.* **2012**, *43* (3), 439−447.
(20) Vtyurin, A. N.; Krylov, A. S.; Goryainov, S. V.; Krylova, S. N.; Oreshonkov, A. S.; Voronov, V. N. *Phys. Solid State* **2012**, *54* (5), 934−936.
(21) Hoang, L. H.; M. Hien, N. T.; Choi, W. S.; Lee, Y. S.; Taniguchi, K.; Arima, T.; Yoon, S.; Chen, X. B.; Yang, I.-S. *J. Raman Spectrosc.* **2010**, *41*, 1005−1010.
(22) Malinovsky, V. K.; Pugachev, A. M.; Surovtsev, N. V. *Phys. Solid State* **2008**, *50* (6), 1137−1143.
(23) Voit, E. I.; Voit, A. V.; Mashkovskii, A. A.; Laptash, N. M.; Kavun, V. Ya. *J. Struct. Chem.* **2006**, *47* (4), 642−650.
(24) Sytko, V. V.; Umreiko, D. S.; Aleshkevich, N. A.; Bokitovko, K. V. *J. Appl. Spectrosc.* **1997**, *64*, 251−257.
(25) Taniguchi, K.; Itoh, Mi.; Fu, D. *J. Raman Spectrosc.* **2011**, *42*, 706−714.
(26) Nakamoto, K. *Infrared and Raman Spectra of Inorganic and Coordination Compound*; John Wiley and Sons: New York, 1986.
(27) Jenkins, T. E. *J. Phys.: Condens. Matter* **1986**, *19*, 1065−1070.